Chem. Soc., Faraday Trans. 2, **80**, 823 and 837 (1984).
8. F. J. Alvarez, *et al., J. Am. Chem. Soc.*, **108**, 6435 (1986).
9. A. G. Mohan, in "Chemi-and Bioluminescence", J. G. Burr(ed.), Marcel-Dekker, New York, 1985, p245, and

references therein.
10. A. G. Mohan and N. J. Turro, *J. Chem. Educ.*, **51**, 528 (1974).

Electrical Conductivity of the System ThO₂-Ho₂O₃

Seung Koo Cho, Sung Ho Park, Keu Hong Kim[*], and Jae Shi Choi

Department of Chemistry, Yonsei University, Seoul 120. Received September 14, 1987

The electrical conductivity of the system ThO_2-Ho_2O_3 was measured in the temperature range 600-1100°C and P_{O_2} range 10^{-5}-2×10^{-1} atm. The mean value of activation energy was 1.45 eV. The observed conductivity dependence on P_{O_2} was $P_{O_2}^{1/4}$ at P_{O_2}'s above 10^{-3} atm and was independent on oxygen partial pressure at P_{O_2}'s below 10^{-3} atm. It is suggested that these dependences are due to a mixed ionic plus electron hole conduction by $V_{\ddot{O}}$ defect.

Introduction

ThO₂ has the fluorite structure up to its melting point[1], while Ho_2O_3 has the rare earth type cubic structure at temperatures lower than 2200°C. The latter changes to hexagonal in the temperature range 2200 to 2300°C[2,3].

ThO₂ was reported to be an n-type semiconductor by Bransky and Tallan[4] at temperatures above 1600°C and P_{O_2}'s below 10^{-8} atm. This n-typeness was also found by Choudhury and Patterson[5] at temperatures below 1400°C and P_{O_2}'s lower than 10^{-20} atm. P_{O_2} dependence of the electrical conductivity in pure ThO₂ has also been reported to vary as $P_{O_2}^{1/5}$[4] and $P_{O_2}^{1/4}$[5-8] at P_{O_2}'s higher than 10^{-3} atm. In addition to the $P_{O_2}^{1/5}$ dependence at P_{O_2}'s higher than 10^{-3} atm, Bransky and Tallan[4] found that the electrical conductivity did not depnd on P_{O_2} for P_{O_2}'s between 10^{-8} and 10^{-3} atm.

From the electrical conductivity, mixed ionic and electronic conductivity was observed[4], and activation energies were reported[4] to be 0.98 eV and 0.77 eV at temperatures from 700 to 1000°C and above 1000°C, respectively. Bransky and Tallan[4] reported that the predominant ionic and electronic charge carriers in ThO₂ were fully ionized metal vacancies and electron holes at P_{O_2}'s above 10^{-8} atm. This defect structure was also reported by Bauerle[8] who attributed his $P_{O_2}^{1/4}$ dependence to the chemical equilibrium between oxygen gas molecules and fully ionized oxygen vacancies. This defect model and that by Subbarao *et al.*[9] differ significantly from the fully ionized metal vacancy found by Bransky and Tallan[4] and from the anti-Frenkel defect *i.e.*, O_i in pure ThO₂ observed by Lasker and Rapp.[6] Hardaway *et al.*[10] reported the maximum electrical conductivity in ThO₂ doped with 7.5 mol % Y_2O_3(15 mol % $YO_{1.5}$) which has already been observed by Lasker and Rapp[6].

In this work ThO₂-Ho₂O₃ systems were prepared, and their electrical conductivities were measured as a function of temperature and P_{O_2}. From the temperature and P_{O_2} dependences of electrical conductivity, one defect model and two carrier types are proposed.

Experimental

Sample preparation. ThO₂ and Ho₂O₃ powders obtained both from the Johnson-Matthey Co. (99.99%) were separately calcinated at 800°C for 6 hr; then weighed, mixed in varying proportions, ballmilled for several hours in C_2H_5OH solution and then dried at 300°C. The powder mixtures were compacted into pellets under a pressure of 48 MPa in vacuum. Pellets of ThO₂ containing 5, 8, 10, 12 mol % Ho₂O₃ were sintered for 48 hr at 1400°C, annealed for 72 hr at the same temperature under atmospheric pressure, and then quenched to room temperature. The pellets were given a light abrasive polish on both faces until voids on the faces were fully eliminated. The specimens were cut into rectangular forms having dimensions of approximately $1.5 \times 0.7 \times 0.4$ cm³. Four holes were drilled into the largest face at intervals of 0.2 cm. The specimens were etched in dilute HNO₃ solution, washed with distilled water, and dried in an oven at 200°C for about 24 hr. As Keller *et al.*[11] and Sibieude and Foex[12] reported, X-ray analysis confirmed that all sintered specimens had ThO₂ type solid solution. Pycnometric densities of specimens are more than 96% of theoretical densities. Spectroscopic analysis of the specimens above showed that total amount of impurity was lower than 20 ppm. Before the sample was introduced into the sample basket, it was always etched in $(NH_4)_2S_2O_8$ and dilute HNO₃, and washed with distilled water, dried, and then connected to the Pt probes.

P₂ establishment. The various oxygen partial pressures were established using pure oxygen or nitrogen or a mixture of 0.001% oxygen in nitrogen obtained from Matheson Gas Products. The quartz sample basket was evacuated to a pressure of 1×10^{-7} torr by a diffusion pump[13] at room temperature, and then the temperature of the sample container was increased up to 200°C. A mixture of oxygen and nitrogen, or pure oxygen, was introduced into the sample basket, which was then evacuated again to a pressure of 1×10^{-6}
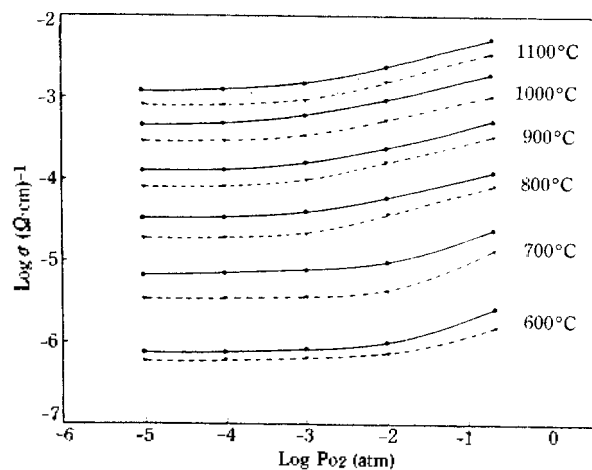
22 *Bull. Korean Chem. Soc., Vol. 9, No. 1, 1988*

Seung Koo Cho et al.
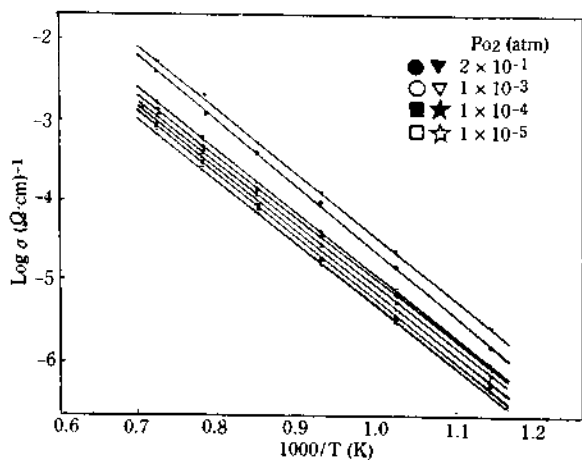
Figure 1. Log conductivity *vs.* 1000/T for 5 mol % (-●- -○--■- -□-) and 8 mol % Ho₂O₃-ThO₂ (- ▼ - -▽ - -★ - -☆ -) under various oxygen pressures.
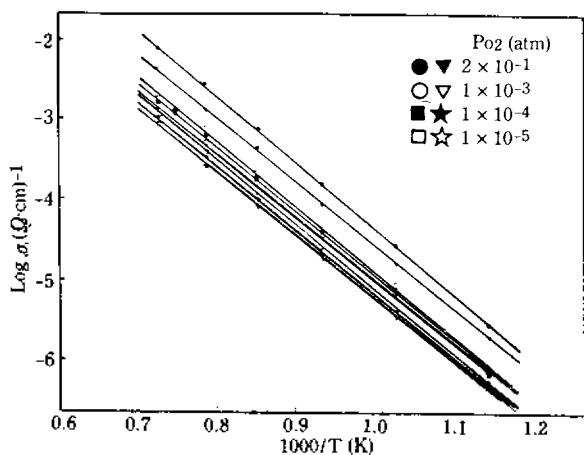
Figure 2. Log conductivity *vs.* 1000/T for 10 mol % (-●- -○--■- -□-) and 12 mol % Ho₂O₃-ThO₂ (- ▼ - -▽ - -★ - -☆ -) under various oxygen pressures.

Figure 3. Log conductivity *vs.* log Po₂ for 5 mol % Ho₂O₃-ThO₂ (- ▼ -)and 8 mol % Ho₂O₃-ThO₂ (-●-) at various temperatures.
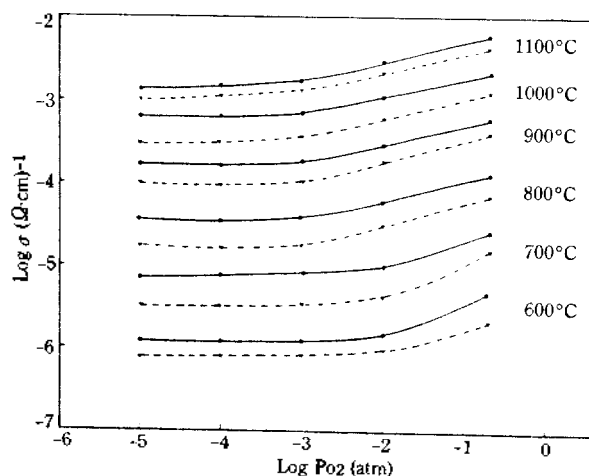
Figure 4. Log conductivity *vs.* log Po₂ for 10 mol % Ho₂O₃-ThO₂ (-●-) and 12 mol % Ho₂O₃-ThO₂ (- ▼ -) at various temperatures.

torr. The introduction and evacuation of gas at 200°C were performed two or three times, and then total pressure was controlled with 0.001% oxygen in nitrogen in order to establish the required Po_2. The pressures of the evacuated sample container and the O_2-N_2 mixture were read on a McLeod gauge, a thermocouple gauge, Pirani gauge, and an ultrahigh vacuum ionization gauge, respectively.

Conductivity measurements. Measurements of electrical conductivity were performed according to the Valdes' technique[14] as described elsewhere[15,16]. This technique has also been employed to measure the electrical conductivity of other oxide semiconductors; for example, α-Fe_2O_3/ Fe_2O_3: $Cd^{17\text{-}20}$, La_2O_3: Cd^{21}, $Sm_2O_3^{22}$, H_2-Reduced Rutile[23], $SrTiO_3$: Ni/Co-Reduced $SrTiO_3$: Ni^{24}, and $Tm_2O_3^{25}$. Details have been described for the vacuum system[26], instruments[27], and the conductivity calculation procedure[15,16]. The sample current was maintained steady at values from 10^{-6} to 10^{-5} A by a rheostat and the corresponding potential drop across the inner two probes was measured; they ranged between 0.2 and 1.8 eV. The potential difference was measured by a Keithley 642 digital multimeter, and the current through the sample was measured by a Keithley 616 digital electrometer. The measurements of electrical conductivity were performed over a cycle in the temperature range 600-1100°C under

Po_2's from 10^{-5} to 2×10^{-1} atm, starting from the low temperature and proceeding toward the high temperature end, and then back again. The sample was held at each temperature until equilibrium between the oxygen phase and sample was achieved, as indicated by a constant conductivity.

Results and Discussion

As shown in Figures 1 and 2, log σ of each sample shows linear dependences on reciprocal temperature from 600-1100 °C with characteristic p-type conduction occurring at Po_2's above 10^{-3} atm. At the Po_2's below 10^{-3} atm, the electrical conductivities of all specimens are nearly independent of Po_2, and an inflection point does not appear. An average activation energy of 1.47 eV is obtained from slopes of log σ *vs.* 1/T at Po_2's above 10^{-3} atm and 1.43 eV is found for Po_2's below 10^{-3} atm. From the analysis of an activation energy, an unique conduction mechanism is expected, however the electrical conductivity dependence on Po_2, as shown in Figures 3 and 4, indicates two possible mechanisms. Log σ *vs.* log Po_2 plots (Figures 3 and 4) were drawn with the data obtained from the log σ *vs.* 1/T plots. Mean slope value in the log σ *vs.* log Po_2 plots for Po_2's above 10^{-3} atm is 1/4 and does not depend on Po_2 at Po_2's below 10^{-3} atm.

Electrical Conductivity of the System ThO_2-Ho_2O_3

Bull. Korean Chem. Soc., Vol. 9, No. 1, 1988 23
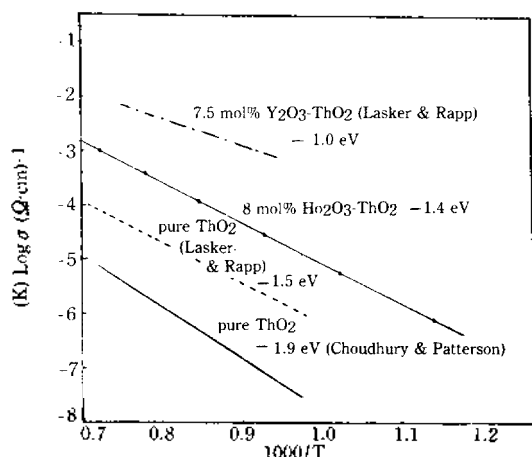
Figure 5. Log conductivity *vs.* 1000/T plots for ionic conductivity of ThO_2, Y_2O_3-ThO_2 and ThO_2-Ho_2O_3 systems.

Figure 6. Log conductivity *vs.* log Po_2 for ThO_2, Y_2O_3-ThO_2 and ThO_2-Ho_2O_3 systems at 1000°C.

As shown in Figure 5, Choudhury and Patterson[5] reported that the ionic activation energy of pure ThO_2 is 1.9 eV. On the other hand, that of pure ThO_2 obtained by Lasker and Rapp[6] is 1.5 eV. This discrepancy was attributed by Choudhury and Patterson[5] to the different amounts of trace impurities that may have been present in the two sets of specimens.

The average activation energy for the ThO_2-Ho_2O_3 system, as determined from slopes in Figures 1 and 2, is below that reported by Choudhury and Patterson[5] for pure ThO_2. This is to be expected because oxygen vacancy conduction in Ho_2O_3 doped ThO_2 should include only the energy for migration. In contrast, the migration energy plus the sizable formation energy for defects would be expected in pure ThO_2 system if it were free enough of impurities. As Wachtman[28] reported for the ThO_2-CaO system, this could be due to a larger amount of energy required to separate the defect pairs in ThO_2-Ho_2O_3 as compared to ThO_2-Y_2O_3.

From the analysis of an activation energy (Figure 5), increasing conductivity with increasing mol % of dopant (Figure 3), and $\sigma \propto Po_2^{1/4}$ (Figures 3 and 4), it is assumed that an oxygen vacancy may be produced by doping with Ho_2O_3. This formation of an oxygen vacancy is represented by the following disorder reaction

$$2\,Ho_{Ho} + 3\,O_o \rightleftharpoons 2\,Ho'_{Th} + V\ddot{o} + 3\,O_4 \tag{1}$$
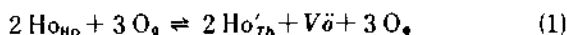
where Ho_{Th}' is effectively negatively singly charged holmium on thorium site and $V\ddot{o}$ is effectively positively doubly charged oxygen vacancy. Provided that gas phase oxygen may react with this oxygen vacancy, the following equilibrium can exist

$$V\ddot{o} + \frac{1}{2}O_2\,(g) \xrightarrow{\ K_1\ } 2h^{\cdot} + O_o \tag{2}$$
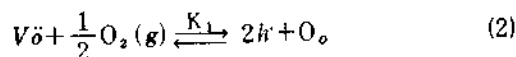
where $h^{\cdot}$ represents electron hole. At equilibrium (2), $K_1 = p^2/(V\ddot{o})Po_2^{1/2}$, where $(V\ddot{o})$ is constant, since $(V\ddot{o})$ is determined by the amount of dopant in disorder reaction (1). One can easily calculate the electron hole concentration: $p = K_1^{1/2}\,(V\ddot{o})^{1/2}\,Po_2^{1/4} = K'\,Po_2^{1/4}$. Since $\sigma \propto p$, the electrical conductivity dependence on Po_2 is $\sigma = p\,e\,\mu = K'e\,\mu\,Po_2^{1/4}$ where e is charge and μ is the mobility. If e and μ are constant, the following equation may be conserved.

$$\sigma = K''Po_2^{1/4} \tag{3}$$

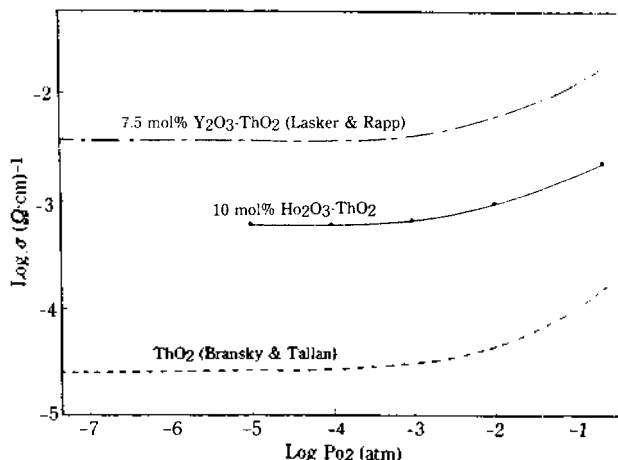This interpretation above equilibrium (2) is in good agree-

ment with experimentally observed conductivity dependence on Po_2, *i.e.*, $Po_2^{1/4}$.

An ionic conductivity is essentially independent on Po_2. It is suggested that an ionic conductivity predominates at Po_2's lower than 10^{-3} atm with respect to Po_2 independence of conductivity. As shown in Figure 6, Lasker and Rapp[6] and Bransky and Tallan[4] interpreted their conductivities as being ionic at Po_2's lower than 10^{-5} atm for 7.5 mol % Y_2O_3-ThO_2 and pure ThO_2, respectively. For 10 mol % Ho_2O_3-ThO_2, the Po_2 range in which ionic conductivity appears is somewhat different, however, it is difficult to determine the correct Po_2 range in which ionic conductivity predominates. This is the reason why it is difficult to determine the precise Po_2 at which ionic conduction changes to electronic conduction, since more likely occuring is continuously changing mechanism over the entire Po_2 range.

ThO_2 has the large interstitial sites whose presence results in interstitial disorder dominating in this lattice, and since the lower Madelung constant results in the binding of anions to their lattice sites being less strong than that of cations, anion Frenkel pairs are the dominant intrinsic defects in ThO_2. Lasker[6] reported that the intrinsic defect of ThO_2 is the anion Frenkel defect. As shown in Figure 6, in pure ThO_2, the conductivity is predominantly ionic at the Po_2 region below 10^{-5} atm. This result might be considered as an intrinsic ionic conduction. The intrinsic ionic conductivity of ThO_2 may be explained by equilibrium (4)

$$O_4 \rightleftharpoons V\ddot{o} + O_i'' \tag{4}$$

where O_i'' is an interstitial oxygen ion and this is assumed to be the main charge carrier for an ionic conduction. In ThO_2-Ho_2O_3 system, an oxygen vacancy is produced by the incorporation of Ho_2O_3 and then neighboring lattice oxygen is transported through this vacancy. This process is represented by the following

$$O_{o1} + V\ddot{o}_2 \rightleftharpoons V\ddot{o}_1 + O_{o2} \tag{5}$$
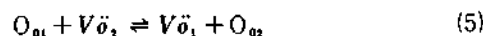
where O_{o1} is lattice oxygen and $V\ddot{o}_2$ is oxygen vacancy formed by Ho_2O_3. With view to energy level, it is assumed that the energy level of interstitial position is higher than that of lattice site. Consequently, the energy required for reaction (4) to proceed to the right is much more than that for required reaction (5). This assumption is well consistent with the experimental result that the activation energy for the electrical con-
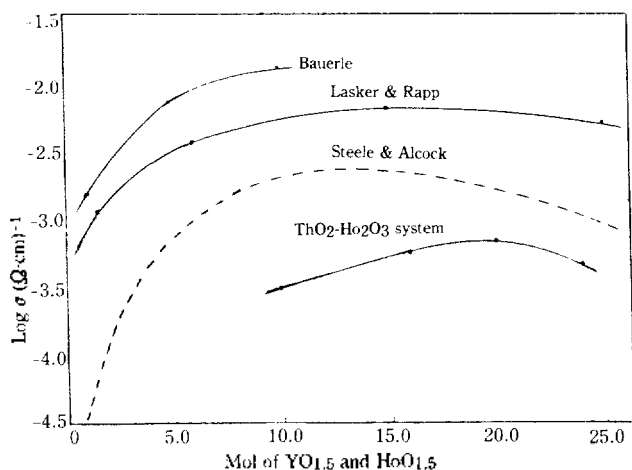
Figure 7. Log conductivity (1000°C) *vs.* mol % of $YO_{1.5}$ and $HoO_{1.5}$ for ionic conductivity of ThO_2-Y_2O_3 and ThO_2-Ho_2O_3 systems.

duction in ThO_2-Ho_2O_3 system is much less than that in pure ThO_2. As shown in Figure 6, since Po_2 dependence of ThO_2-Ho_2O_3 is smaller than pure ThO_2 and the magnitude of the ionic conductivity of ThO_2-Ho_2O_3 system is larger than that of pure ThO_2, it is reasonalbe to say that the oxygen vacancy concentration produced by doping with Ho_2O_3 is larger than that in pure ThO_2. It is concluded that the main defect for ionic conduction is an oxygen vacancy produced by doping with Ho_2O_3 at Po_2's lower than 10^{-3} atm.

Assuming an ideal solution model, disorder reaction (1) predicts that the ionic conductivity in ThO_2-Ho_2O_3 system would be proportional to the doping ratio of Ho_2O_3, but as shown in Figure 7, it is not a linear function when Ho_2O_3 content increases further: The conductivity increases with increasing Ho_2O_3 content up to about 10 mol % Ho_2O_3 where it goes to a maximum and then decreases with additional doping of Ho_2O_3. In Figure 7, it can be seen that ThO_2-Y_2O_3 system[6,8,31] have the same tendencies as ThO_2-Ho_2O_3 system. The lowering of conductivity of 12 mol % Ho_2O_3-ThO_2 system may originate from decreasing mobility of oxygen ion due to the formation of vacancy ordering[33] or dopant-vacancy interaction[34].

Conclusion

The activation energy for an ionic conduction is almost equal to that for an electronic conduction, however, an ionic conductivity is suggested at oxygen partial pressures lower than 10^{-3} atm from σ independent on Po_2 and an electronic conductivity is confirmed at oxygen partial pressures higher than 10^{-3} atm with $\sigma \, \alpha \, Po_2^{1/4}$.

The ThO_2-Ho_2O_3 systems investigated have identical defect, $V\ddot{o}$, with two different conduction mechanisms, *i.e.*, ionic and electronic.

The charge carriers are an oxygen anion for the ionic conductivity and an electron hole for the electronic conductivity, respectively.

References

1. D. M. Roy and R. Rustum, *J. Electrochem. Soc.*, **111**, 421 (1964).
2. M. Foex and J. P. Traverse, *Rev. Int. Hautes Temper. Refract.*, **3**, 492 (1966).
3. R. S. Roth and S. J. Scheider, *Res. Natl. Bur. Std.*, **64A**, 309 (1960).
4. I. Bransky and N. M. Tallan, *J. Am. Cer. Soc.*, **53**, 90 (1970).
5. N. S. Choudhury and J. W. Patterson, J. Am. Cer. Soc., **57**, 90 (1974).
6. M. F. Lasker and R. A. Rapp, *Z. Phys. Chem.*, **49**, 198 (1966).
7. C. Wagner, *Z. Physik. Chem.*, **B22**, 181 (1933).
8. J. E. Bauerle, *J. Chem. Phys.*, **45**, 4162 (1966).
9. E. C. Subbarao, P. H. Sutter and J. Hrizo, *J. Am. Cer. Soc.*, **48**, 443 (1965).
10. J. B. Hardaway, J. W. Patterson, D. R. Wilder and J. D. Schieltz, *J. Am. Cer. Soc.*, **54**, 94 (1971).
11. C. Keller, U. Berndt, H. Engerer and L. Leitner, *J. Solid State Chem.*, **4**(3), 453 (1972).
12. F. Sibieude and M. Foex, *J. Nucl. Mater.*, **56**(2), 229 (1975).
13. J. S. Choi, K. H. Kim and S. R. Choi, Inter. *J. Chem. Kinet.*, **9**, 489 (1977).
14. L. B. Valdes, *Proc. IRE*, **42**, 420 (1954).
15. J. S. Choi, H. Y. Lee and K. H. Kim, *J. Phys. Chem.*, **77**, 2430 (1973).
16. J. S. Choi, Y. H. Kang and K. H. Kim, *J. Phys. Chem.*, **81**, 2208 (1977).
17. K. H. Kim, H. S. Han and J. S. Choi, *J. Phys. Chem.*, **83**, 1286 (1979).
18. K. H. Kim and J. S. Choi, *J. Phys. Chem*, **85**, 2447 (1981).
19. K. H. Kim, D. Kim and J. S. Choi, *J. Catalysis*, **86**, 219 (1984).
20. K. H. Kim, S. H. Lee and J. S. Choi, *J. Phys. Chem. Solids*, **46**, 331 (1985).
21. K. H. Kim, S. H. Lee and Y. R. Kim and J. S. Choi, *J. Catalysis*, **88**, 283 (1984).
22. K. H. Kim, H. J. Won and J. S. Choi, *J. Phys. Chem. Solids*, **45**, 1259 (1984).
23. K. H. Kim, E. J. Oh and J. S. Choi, *J. Phys. Chem. Solids*, **45**, 1265 (1984).
24. K. H. Kim, K. H. Yoon and J. S. Choi, *J. Phys. Chem. Solids*, **46**, 1061 (1985).
25. J. S. Choi, K. H. Kim and W. Y. Chung, *J. Phys. Chem. Solids*, **46**(10), 1173 (1985).
26. J. S. Choi and K. H. Yoon, *J. Phys. Chem.*, **74**, 1095 (1970).
27. J. S. Choi and K. H. Kim, *J. Phys. Chem.*, **80**, 666 (1976).
28. J. B. Wachtman Jr., Phys. Rev. **131**, 517 (1963).
29. Per Kofstad, "Nonstoichiometry, Diffusion and Electrical Conductivity in Binary Metal Oxides", Wiley-Interscience, New York, 1972.
30. R. J. Eckermann, E. G. Rauh, R. J. Thorn and M. C. Cannon, *J. Phys. Chem.*, **67**, 762 (1963).
31. B. C. H. Steele and C. B. Alcock, *Trans. AIME*, **223**, 1359 (1965).
32. H. S. Maiti and E. C. Subbarao, *J. Electrochem. Soc.*, **123**, 1713 (1965).
33. T. Y. Tien and E. C. Subbarao, *J. Chem. Phys.*, **39**, 1041 (1963).
34. F. A. Kröger, *J. Am. Cer. Soc.*, **49**, 215 (1966).